Acta Cryst. (1981). B**37**, 2123–2132

Electronic Structures of Solids from a Simple Viewpoint: Some Structures Derived from the Cesium Chloride Arrangement

BY JEREMY K. BURDETT AND JUNG-HUI LIN

Department of Chemistry, The University of Chicago, Chicago, Illinois 60637, *USA*

(*Received* 18 *September* 1980; *accepted* 21 *April* 1981)

Abstract

Molecular-orbital techniques well established in the theoretical analyses of the electronic structures of molecules are used to study the structures of some solid-state systems. By analogy with four-coordinate molecules, the CsCl structure, shown to be stable for eight electrons per AX unit, is found to be potentially unstable for the ten-electron case and a distortion may result (*e.g.* to red PbO). The tendency to distort increases with the AX electronegativity difference. In molecular-orbital language the central atom of the CsCl structure is isolobal with a regular tetrahedron of atoms and the electronic structure of an MA_4 species, where a tetrahedron is placed inside a primitive cubic cell, is examined. A stuffed tetrahedron behaves analogously and the cuprite structure results. The site preferences in this structure are found to be dependent on the total electron count. The CaB_6 structure is approached in a similar way and the possibility of defect structures investigated.

Introduction

Simple molecular-orbital ideas of widespread application and utility now have a well established place in molecular inorganic and organic chemistry. Perturbation theory, the fragment formalism and the isolobality concept, and ways to understand molecular geometry, barriers to rotation and ligand-site preferences have all contributed to a global understanding at a very fundamental level to the molecular scene (Burdett, 1980*b*; Hoffmann, 1981; Mingos, 1977). We have previously used some of these ideas in the solid-state context to view the geometrical arrangements of atoms in solids in a hitherto unexplored way (Burdett, 1979, 1980*b*). In this paper we investigate further the application of these techniques to the structure of solids. In principle the electronic structure of these materials should be approached using band theory to appreciate fully the infinite three-dimensional connectivity of the structure. Although we shall actually discuss one of our studies using this formalism, the gross electronic features of these particular systems may sometimes be quite well understood by an investigation of the level structure of the orbitals of a repeat unit with cyclic boundary conditions imposed to mimic the local solid-state environment, although there are many areas where consideration of the full band structure is vital. As we have shown elsewhere, these fragment-within-the-solid orbitals for a single repeat unit represent those of the band structure at the point $\Gamma(\mathbf{k}=0)$ (Burdett, 1980*c*). The method has also been called the small-periodic-cluster technique (Zunger, 1974, 1975) and the molecular-unit-cell approach (Messmer, McCarroll & Singal, 1972; Messmer & Watkins, 1973; Watkins & Messmer, 1973). We shall use Extended Hückel (Hoffmann & Lipscomb, 1962) molecular-orbital calculations to underwrite our, mainly symmetry-based, ideas and to generate diagrams of this type. The parameters used are given in the Appendix. We do remind the reader, however, that relative to some of the molecular-orbital methods available the method is very crude and its numerical results are not always to be trusted. In spite of this qualification its careful use has made a vital contribution to our understanding of molecular organic and inorganic chemistry by highlighting the symmetry and overlap arguments upon which the majority of qualitative ideas are based.

The CsCl and red PbO structures

The very simple CsCl structure (1) consists of a single A or X atom located at the centroid of a cube of atoms of the opposite type. Both A and X are in eightfold coordination, a geometry which is not very common in molecular systems but quite prevalent in the extended solid state.

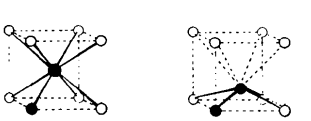

(1) (3)

0567-7408/81/122123-10$01.00

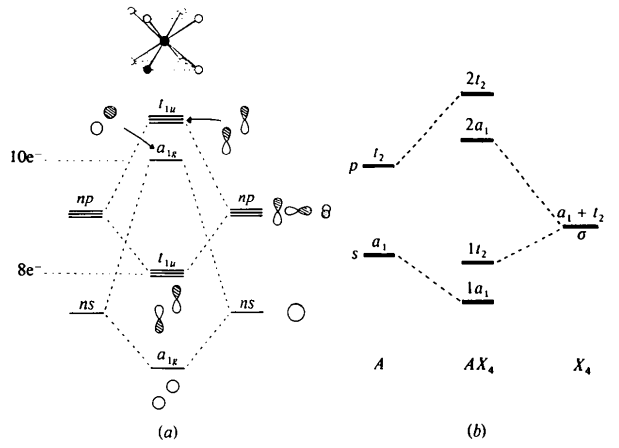

Fig. 1. (*a*) The fragment-within-the-solid orbitals of the CsCl structure. (*b*) A σ-only molecular-orbital diagram for a tetrahedral AX_4 molecule.

The smallest repeat unit of the structure is clearly the pair of atoms at 0,0,0 and $\frac{1}{2},\frac{1}{2},\frac{1}{2}$. An orbital diagram for this diatomic AX fragment-within-the-solid is shown in Fig. 1 and is generated by using the cyclic boundary conditions (Burdett, 1980*c*) or the small-periodic-cluster method (Zunger, 1974, 1975). (It represents the band-structure energies at the point Γ of the Brillouin zone, $\mathbf{k} = 0$.) Triply-degenerate t_{1u} bonding and antibonding orbitals are found *via* *p–p* overlap and a corresponding pair of a_{1g} orbitals arise from *s* orbital overlap, as required by the local cubic environment of both atoms. In fact the form of the diagram is the same for all three cubic coordination geometries found in CsCl, rocksalt and sphalerite. Fig. 1 also shows the form of the a_{1g} orbitals and one component of the t_{1u} orbitals. The diagram bears a striking resemblance to that shown in Fig. 1(*b*) for a tetrahedral molecule (*e.g.* CH_4), a relationship we will find very useful in our treatment below.

All the low-energy orbitals in this solid-state structure are occupied with a total of eight electrons per AX unit as found in CsCl itself. For octet main-group *molecules* such as CH_4 and CF_4 the analogous collection of orbitals are also occupied. Note the large HOMO(highest occupied molecular orbital)–LUMO (lowest unoccupied molecular orbital) gap for molecules with this configuration, a feature which bestows structural and often kinetic stability on a molecular species. For ten-electron systems the antibonding a_{1g} (in the solid) or a_1 (in the tetrahedral molecule) is doubly occupied. In the molecular case with a total of five valence electron pairs (*e.g.* SF_4) the tetrahedral geometry is now unstable and the molecule is found in a C_{2v} geometry (2).

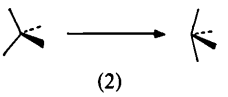

(2)

This may be understood by using a variety of theoretical approaches ranging from the VSEPR approach to molecular-orbital arguments. Of particular interest to us is the mixing of HOMO and LUMO of the parent structure as the result of a perturbation (distortion of the molecule). Often described under the umbrella of the second-order Jahn–Teller approach (Hoffmann, 1971; Bartell, 1968; Pearson, 1969, 1970) we need to find that distortion coordinate which effectively mixes HOMO and LUMO, leads to a dramatic stabilization of the former (if the HOMO–LUMO energy gap is small) and perhaps of the whole system on distortion. Because of the symmetry species of HOMO and LUMO for SF_4 at the tetrahedral structure a distortion of symmetry t_2 is predicted as in (2) and the HOMO–LUMO gap in the distorted structure is larger than that in the parent. For the solid-state system analogous arguments apply. Such ideas have not been widely used in this area but it is interesting to recall that Heine & Weaire (1970) noted that the sometimes distorted structures of metals are those where the lattice vectors have moved so as to increase the band gaps. One possible distortion for the ten-electron system is movement of an atom towards a face of the cube as in (3) to give the local geometry of the red PbO structure. Our numerical calculations are not definitive in predicting the most energetically favorable distortion route, since it involves bond-length changes which the method usually does not match very well. Generally, however, for a range of orbital parameters for A and X we find that distortion towards the face is favored over other unit displacements towards an edge or corner. With a specific phase relationship between the distortions of adjacent cells the red PbO structure of Fig. 2 results. [The yellow form of PbO is obtained by puckering the X(O) atoms of the red structure.]

We are particularly interested in a population analysis of this distorted structure in order to see which out of the A (electropositive) or X (electronegative) atoms will occupy the two distinctly different sites. In molecular studies, ligand-site preferences are often approachable [see, for example, Burdett (1980*a*) and Hoffmann, Howell & Rossi (1976)] by placing the most electronegative ligand at the site of largest electron density in the unsubstituted parent. One site in

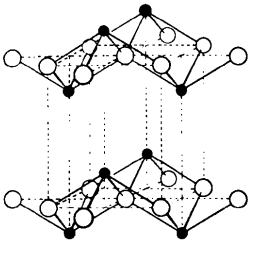

Fig. 2. The red PbO structure.

red PbO has a tetragonal-pyramidal coordination (occupied by Pb), the other is tetrahedrally coordinated (occupied by O). Such an analysis of the fragment-within-the-solid orbitals for an A_2 system with this geometry shows that the charge is highest on the tetrahedrally coordinated atom at 0,0,0. (We use identical atomic-orbital parameters for the two different types of atoms so as not to bias the result, just as in analogous molecular studies.) Thus the most electronegative atom (in this case O) is predicted to occupy this position. The least electronegative atom (Pb) is predicted to occupy the tetragonally coordinated site. These predictions are borne out nicely in the actual structure.

Given this atomic disposition in the distorted structure we can use simple perturbation-theory arguments to see how the HOMO and LUMO of the CsCl structure mix together to produce the HOMO of the red PbO structure. Because of the electronegativity difference between Pb and O the higher-energy a_{1g} and t_{1u} orbitals are largely Pb located and their lower-energy (bonding) counterparts appear largely O located. Clearly, Fig. 3 shows that one component of $2t_{1u}$ mixes into $2a_{1g}$ to produce a lone-pair orbital which points out of the top of the tetragonal pyramid as in (4). On an orbital basis the result is very similar to that found for the SF_4 molecule (Burdett, 1981). Elsewhere (Burdett, Haaland & McLarnan, submitted for publication) we examine theoretically the electronic structure of the arsenic layer structure, where each atom is trigonally pyramidally coordinated with a lone pair occupying the vacant tetrahedral position (5).

(4) (5)

This arrangement may be viewed as being derived from that of rocksalt by breaking three mutually perpendicular linkages (*e.g.* Wells, 1975) around each atom, as the result of the addition of two extra electrons. In our present example the result of the incorporation of an extra two electrons into the CsCl structure has been the fission of four of the eight cubal linkages around each center and the generation of a lone pair of electrons in an analogous way. This tetragonal-pyramidal structure is a relatively rare one for molecules, found for example in (diethylthiocarbamato)lead(II) (Giricheva, Zasorin, Girichev, Krasnov & Spiridonova, 1976), but is found in several solid-state systems such as the isoelectronic Bi^{III} oxides. In BiOF where $Bi^{III}O_4$ pyramids are found arranged in a similar way to those in red PbO, the fluorine atoms (ions) occupy positions between the layers (*e.g.* Andersson & Åström, 1972).

There are two other (unobserved) simple variants of the distorted CsCl structure which bear examination.

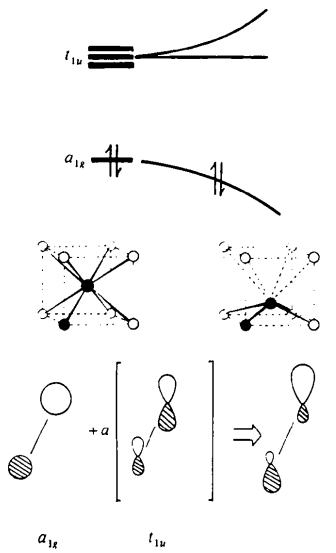

Fig. 3. HOMO–LUMO mixing of the orbitals of Fig. 5 to give a lone-pair orbital.

Within a contiguous block of four CsCl cubes, the movement of one of the central atoms may be either in- or out-of-phase with respect to that in the next cell. (6) shows the observed structure of Fig. 6, and (7) and (8) show two other possibilities. (The solid circles represent central atoms displaced downwards, the open circles atoms displaced upwards.)

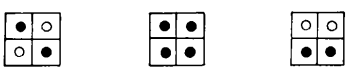

(6) (7) (8)

Whereas (6) leads to tetrahedral O coordination, (7) and (8) lead to tetragonal-pyramidal and square-planar O environments respectively. Since the OPb_4^{6+} fragment on VSEPR grounds has four valence electron pairs around the O atom, the stability of the tetrahedral structure over the other two is not surprising. Indeed, calculations on such fragments, using the parameters given in the Appendix, employed both in the fragment-within-the-solid orbitals and the band-structure calculations below, show that this structure is most stable. (We do, however, discuss the influence of parameter choice on this result in the Appendix.)

The band structure of red PbO

Here we see how the results of the previous section fit in with band-structure calculations on the CsCl and red PbO structures. The band structure of the CsCl structure is quite simple and is shown in Fig. 4(*a*). It was obtained by using the same atomic-orbital parameters as in the previous section and the solid-state equivalent of the LCAO method, the 'tight-binding' approach, was used to construct the levels. We start by

viewing the structure of CsCl as being derived from two interpenetrating primitive cubic lattices (*e.g.* Harrison, 1980). For a single lattice of this type the dependence of the orbital energy on the wavevector **k** is very simply derived. Considering first-nearest-neighbor contacts for *s* orbitals alone, the energy is found (*e.g.* Reitz, 1955) to vary as in Fig. 5(*b*), with the energies at the symmetry points of the Brillouin zone specifically depicted. For a body-centered cubic lattice (with identical atoms at both sites) the **k** dependence of the *s* bands (there are two basis orbitals in the problem) is shown in Fig. 6(*a*). When the two atoms of this structure are different (and have different values of the Coulomb integral H_{ss}) then these bands split apart in energy as shown in Fig. 6(*b*). The behavior of the lowest energy *s* band from the calculated band structure of Fig. 4(*a*) is in fact very similar to a weighted version of Fig. 5(*b*) and the lower half of Fig. 6(*b*) with the dominant interaction arising along the edges of the cell. The differences are due to *sp* mixing at points in the zone where the symmetry is low enough to allow it.

There is a simple reason for the dominance of this picture by edge interactions. First the distance between the atoms at the corners of the cell is only 15% greater than the distance between the atoms located at the corner and cell center. Secondly, the electronegativity difference between the orbitals on the two different atoms along the body diagonal implies a smaller interaction (for a given distance) than that between the edge atoms. Often the effect of the coupling of the band structures of the two interpenetrating primitive cubic lattices is tackled by using perturbation theory (*e.g.* Harrison, 1980).

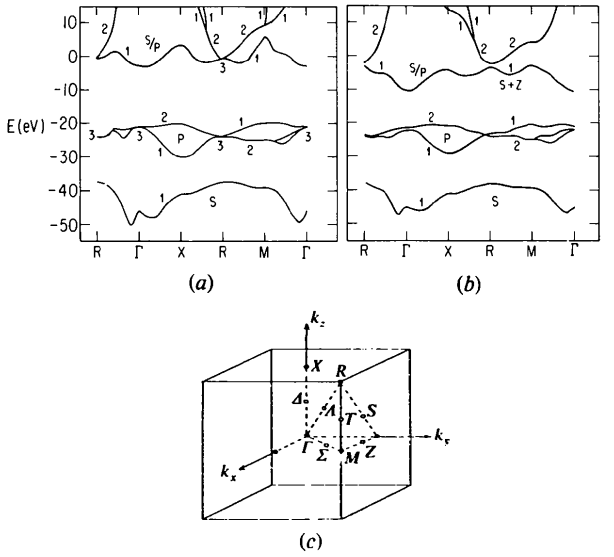

Fig. 4. (*a*) The band structure for the CsCl structure. (*b*) The band structure of red PbO. (*c*) The symmetry points of the Brillouin zone for a primitive cubic Bravais lattice. The small numbers indicate the degeneracy of the levels.

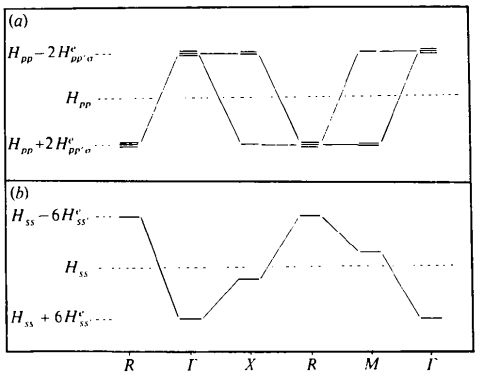

Fig. 5. The **k** dependence for a primitive cubic lattice of the energy of (*a*) the *p* orbitals and (*b*) the *s* orbitals.

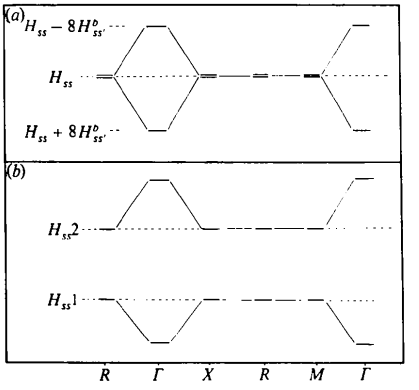

Fig. 6. The **k** dependence of the energy of the *s* orbitals of a body-centered cubic lattice with (*a*) identical and (*b*) different values of H_{ss} for the two atoms of the repeat unit.

The behavior of the *p* orbitals is a little more tricky to derive analytically but at high-symmetry points [*e.g.* $\Gamma(0,0,0)$ and $R(\frac{1}{2},\frac{1}{2},\frac{1}{2})$] the three orbitals remain triply degenerate by symmetry. At other points the degeneracy is either partially or totally lifted. The calculated features of the lowest *p* band of Fig. 4(*a*) actually match quite well the analytic function for a primitive cubic lattice shown schematically in Fig. 5(*a*).

For the higher-lying bands an interesting effect occurs. We would perhaps expect similar behavior to that for the *s* and *p* bands just described. At the point $\Gamma(0,0,0)$ the *s* band receives its maximum stabilization (Fig. 5*b*) and its maximum destabilization at the point $R(\frac{1}{2},\frac{1}{2},\frac{1}{2})$. The converse is true of the *p* orbitals (Fig. 5*a*). At Γ, dominated by the superiority of σ over π interactions (a larger σ compared to π resonance integral) the maximum destabilization of the *p* band is felt and the maximum stabilization is realized at the point *R*. From separate calculated *E versus* **k** plots of the *s* and *p* orbitals of the system we find that in numerical terms the *s* and *p* bands actually cross somewhere between Γ and *R* as shown schematically in Fig. 7(*a*). Because of *sp* mixing such crossing does not

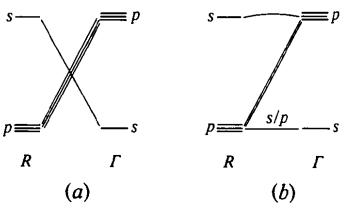

Fig. 7. Illustration of the avoided crossing of the higher-energy s,p bands of the CsCl structure, (*a*) no *sp* mixing, (*b*) with *sp* mixing.

occur in practice in the real system and the highest-energy occupied orbital, pure s at Γ, smoothly changes in character to pure p at the point R. Thus the valence band is non-degenerate (either pure s or an sp mixture depending on symmetry) at all points other than R. Here it is pure p in character and triply degenerate. On distortion from CsCl to red PbO this triply-degenerate set of orbitals at R split apart in energy as the symmetry is lowered to give a small energy gap (calculated to be about 1·2 eV), probably responsible for the color of the material (Fig. 4*b*). The other band gaps are much larger. Numerically, the stabilization of the structure on distortion is dominated by the stabilization of the valence band as shown in Fig. 4(*a*,*b*).

Chadi & Cohen (1973) and Baldereschi (1973) have devised the special-points method for evaluating the energy or charge density *etc.* of a solid-state system for those cases (as ours) where there are no partially filled bands. Instead of integration of $E(\mathbf{k})$, the total energy is often well given by that at one special point ($\frac{1}{4},\frac{1}{4},\frac{1}{4}$ in the primitive cubic case) or the weighted average of that of a small collection of special points. This saves the integration $E(\mathbf{k})$ over $\mathbf{k}$ and enables access to the main electronic features of the system from a single calculation. From Fig. 4(*a*,*b*) there is clearly a good energetic stabilization on distortion at this point dominated by the behavior of the 'HOMO'. An analysis of the nature of the valence band at this point also shows generation of the lone-pair orbital shown in (4), on distortion of the structure from CsCl to red PbO just as described above for the fragment-within-the-solid orbitals.

The inert-pair effect

In some ten-electron systems, TlBr and TlCl for instance in contrast to PbO, undistorted geometries are found. This inert-pair effect has recently been rationalized by noting (Pitzer, 1979) that relativistic corrections, expected to be non-negligible for elements of high Z, lead to a 'contraction' of both s and p orbital wavefunctions, but with a much larger effect for the former. (Our numerical calculations have attempted to mimic this state of affairs by using a more contracted s orbital wavefunction.) It has long been recognized that the effect cannot exclusively be explained on the basis of ionization enthalpies (*e.g.* Cotton & Wilkinson, 1980). We can immediately see how such contraction leads to structural impotency for the ns^2 pair of electrons. HOMO–LUMO mixing arises *via* overlap of the p orbitals on one atom with the s orbital on the other which is forbidden by symmetry (at Γ) for the CsCl arrangement. If the s orbital is contracted, to the extent that such coupling is small, then stabilization of the HOMO by this mechanism will not occur and the structural stability of the ten-electron species will be similar to that of systems with eight electrons.

It is noteworthy that those heavy-atom ten-electron systems which are distorted contain small electronegative atoms (*e.g.* PbO, SnO with distorted structures compared to TlCl and TlBr with undistorted ones). The stereochemical effect of the small atoms is often ascribed to their 'polarizing' power but there is an orbital-based explanation for this observation. As the electronegativity of the X atom in the AX system increases, we find that the antibonding t_{1u} orbital set of Fig. 5 drops to lower energy and the HOMO–LUMO gap gets smaller, commensurate with a larger energy stabilization when viewed in perturbation-theory terms. Similar arguments have also been used to rationalize the bond angles in AX_2 and AX_3 molecules as the electronegativity of X increases (Bartell, 1968). Systems with the largest distortion away from the linear or trigonal-planar geometries are those where X has the highest electronegativity. A related energy-gap argument has also been used to understand the structural stability of square-planar XeF_4 compared with the flexibility of octahedral XeF_6 (Bartell, 1968).

The structures of the AX systems TlBr and TlCl (undistorted CsCl) and those of SnO and PbO (distorted CsCl) are well resolved on a structural plot (St John & Bloch, 1974; Zunger, 1980*a*,*b*) using combinations of density functional radii r_s, r_p. The distorted structures have larger values of the parameter $R_\sigma^{AX} = |(r_p^A - r_p^X) + (r_s^A - r_s^X)|$ which appears to vary largely due to changes in the p orbital function. It is pertinent to tie this result to our discussion. If we consider two orbitals with Coulomb integrals H_{ii} and H_{jj}, then the interaction energy is simply given by perturbation theory as

$$\Delta E = \frac{H_{ij}^2}{H_{ii} - H_{jj}}. \qquad (1)$$

Using the geometric-mean Wolfsberg–Helmholz formula for the resonance integral $H_{ij} = K(H_{ii}H_{jj})^{1/2}S_{ij}$ where S_{ij} is the overlap integral then

$$(\Delta E)^{-1} = (K^2 S_{ij}^2)^{-1}\left(\frac{1}{H_{jj}} - \frac{1}{H_{ii}}\right). \qquad (2)$$

Identifying the H_{ii} values as valence-state orbital-ionization energies and noting that Zunger's (1980*b*) r_i

values inversely correlate with such atomic parameters then

$$(\Delta E)^{-1} \propto r_p^A - r_p^X, \qquad (3)$$

where we specifically identify the orbitals i and j as being p orbitals located on the atoms A and X. Thus, either as the ligand electronegativity increases in the Mulliken sense [H_{ii} increases in equation (2)], or as the Zunger index $|r_p^A - r_p^X|$ increases, distorted CsCl structures are observed. We described this result in orbital terms above; as the electronegativity of the X atom increases, the antibonding p orbital manifold drops to lower energy [smaller ΔE in equation (2)] and the HOMO–LUMO gap decreases. It will be interesting to see if similar orbital explanations are a useful way to analyze the chemical features behind the structural plots in general.

The cuprite structure

One of the powerful techniques of modern molecular theoretical inorganic chemistry is the use of the fragment formalism in assembling complex structures from simpler fragments (Burdett, 1980*a*; Hoffmann, 1981). We have shown how the method can be used in the solid state by assembling a variety of structures from puckered arsenic-type sheets (Burdett, 1980*b*). All one needs are the frontier orbitals of the fragments (*i.e.* those that are important in interactions with other units) followed by a study of their energetic behavior as the complex molecule is assembled. In this way we can often identify the electronic reasons for the stability of one particular geometry over another. One very useful outcome of the application of this technique is the observation that as far as their frontier orbitals are concerned many pairs of fragments are both isoelectronic and isolobal (Halpern, 1968; Mingos, 1977). These terms mean that the frontier orbitals of the two units are similar in spatial extent and energy and contain the same number of electrons. For example, the C–H or C–R fragment is isolobal and isoelectronic with the transition-metal carbonyl fragments, $Co(CO)_3$ and $Ir(CO)_3$ (*e.g.* Mingos, 1977). The frontier orbitals located on the carbon or metal atom respectively are very much alike. This implies that C–R and $Co(CO)_3$ should form similar types of molecules. Indeed, the organometallic analog of the tetrahedrane derivative C_4R_4 (9) is known as $Co_4(CO)_{12}$ which contains (10) a tetrahedron of cobalt atoms, just as C_4R_4 contains a tetrahedron of carbon atoms. There is, in fact, a whole isostructural series $[M(CO)_3]_n[CR]_{4-n}$ for $n = 0$–4.

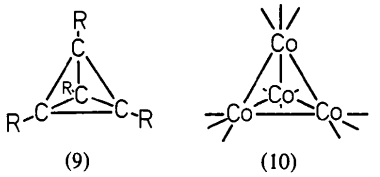

(9) (10)

In the present case we may inquire whether there are other structural units with suitably located frontier orbitals which may replace the central atom of the CsCl structure to give a stable arrangement. It may be recalled that the orbitals of the fragment-within-the-solid for CsCl in Fig. 4 or the band structure itself are derived from a triply-degenerate set of p orbitals, plus a deeper-lying s orbital located on the central atom. One unit which has a similar frontier-orbital structure to that of the isolated atom is the tetrahedron. Fig. 8 shows the level ordering and description for this polyhedral arrangement (*e.g.* Kettle, 1960). Of the sixteen molecular orbitals (s, p on each atom), six are involved in σ bonding within the framework, six are involved in analogous antibonding interactions and four are outward-pointing hybrid orbitals. In the free P_4 molecule with 20 electrons, all the skeletal bonding orbitals are filled, giving rise to six two-center two-electron bonds. The four outward-pointing orbitals are also full and here are best described as lone pairs. It is these outward-pointing orbitals which, using the isolobality concept, may play the same electronic role in the structure of an AX_4 system (11) as those of the central-atom orbitals in the CsCl structure itself.

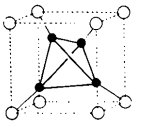

(11)

Fig. 9 shows the generation of the fragment-within-the-solid orbitals for the tetrahedron within the cube. The largest energy changes are associated with the a_1 and t_2 orbitals of the corner atom of the primitive cube and these outward-pointing tetrahedron orbitals. Just as in P_4 itself a total of 20 electrons are needed in this AX_4 structure for it to be stable. We have not been able to find an example of such an arrangement but the orbitals of the stuffed tetrahedron, however, are quite

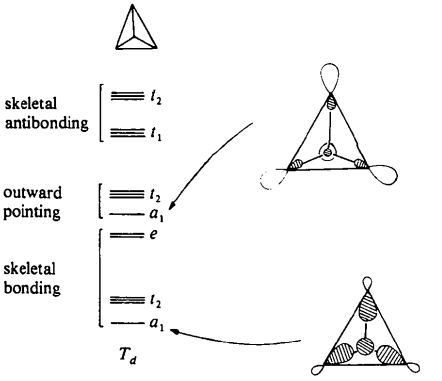

Fig. 8. The energies and spatial extent of the orbitals of a tetrahedron of atoms. The inward- and outward-pointing orbitals of a_1 symmetry are shown specifically.

similar to those of the simple tetrahedron (Fig. 10). Insertion of such an A_4X unit into a primitive cube of X atoms leads to the cuprite structure (12) found for Cu_2O and Ag_2O.

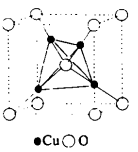

(12)

This system may also be regarded (Pearson, 1972) as a defect superstructure of cubic diamond (actually, the chalcopyrite structure minus the iron atoms) or as two independent, interlocking β-cristobalite-type frameworks. Fig. 11 shows the generation of the fragment-within-the-solid orbitals of cuprite. (We will describe the assembly of the band structure of Cu_2O elsewhere.) Of importance is that in this structure, only the Cu—O bonding orbitals are filled for the Cu_2O electronic configuration. The Cu—Cu bonding orbitals, the skeletal bonding orbitals of the tetrahedron, remain empty, consistent with the rather long Cu—Cu distances. Thus the two interpenetrating β-cristobalite frameworks are not connected to each other by strong bonds at least. For Cu_2O the Cu—O and Cu—Cu bond-overlap populations are calculated to be 0·63 and 0·005 respectively. For this system, the lowest eight orbitals are occupied and a sizable HOMO–LUMO gap of about 3 eV is found.

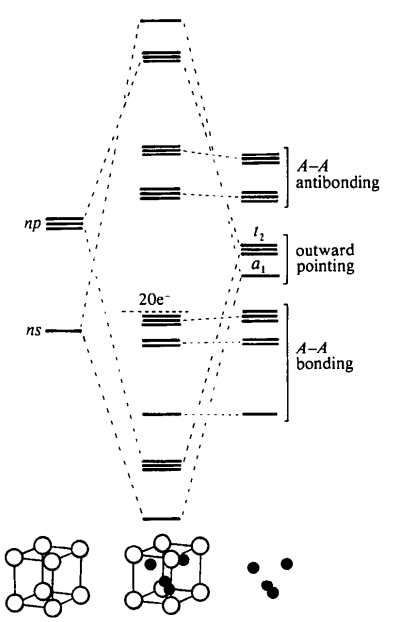

Fig. 9. The generation of the fragment-within-the-solid orbitals of the structure obtained by placing a tetrahedron inside a primitive cube of atoms. Note that the only orbitals of the tetrahedron which change in energy significantly are those which are outward pointing in Fig. 8.

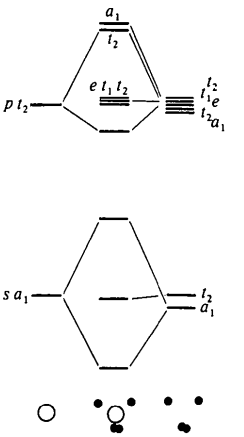

Fig. 10. The orbitals of the stuffed tetrahedron. Here the distances between the atoms of the tetrahedron are longer than in Figs. 8 and 9, so that interactions between the orbitals on these atoms are smaller than before. The interaction of the orbitals of the central atom is exclusively with the 'inward and outward' pointing a_1 and t_2 sets of orbitals of Fig. 8.

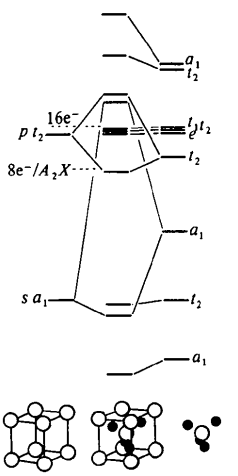

Fig. 11. The generation of the fragment-within-the-solid orbitals of the structure obtained by placing a stuffed tetrahedron inside a primitive cubic cell of atoms. The corner-atom s,p orbitals interact significantly with more of the stuffed-tetrahedron orbitals than in the case shown in Fig. 9 since the skeletal-bonding and inward-pointing orbitals of Fig. 8 have a much larger density outside of the tetrahedron when it contains a central atom.

In order to examine the site preferences in this system, we performed a population analysis on the results of a molecular-orbital calculation where the atomic-orbital input parameters were the same. (13) and (14) show the results for eight-electron (*e.g.* Cu_2O) and sixteen-electron systems.

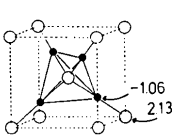

(13)

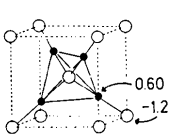

(14)

For the former, the least electronegative atom (Cu or Ag) is predicted to occupy the two-coordinate sites and the more electronegative atom (O) the four-coordinate sites, as actually found in the structure. For the sixteen-electron species, the opposite prediction is made and, while there are no AX_2 systems which adopt this structure, the anticuprite structure is indeed found for $Zn(CN)_2$ and $Cd(CN)_2$. A similar reversal of site preferences between eight- and sixteen-electron systems was discussed in our earlier study of the cadmium halide structures (Burdett, 1980*b*). In general, the molecular rule of thumb, that the most electronegative atom will occupy the site of lowest coordination, is only obeyed in these solid-state examples by the sixteen-electron systems. Given this state of affairs we should look for AX_4 species with twenty electrons containing an A atom that is more electronegative than X. We also note that, viewed as a double-defect diamond derivative superstructure the cuprite structure does not obey the Grimm–Sommerfeld valence rule but has an average of two electrons per site (Burdett, 1981).

For simplicity we have only included s,p orbitals on the metal in these calculations. Inclusion of d orbitals changes little the qualitative results of the preceding paragraphs. Cu–Cu interaction increases by a small amount due to mixing of the metal d orbitals with higher-energy metal orbitals. Decreased Cu^I–Cu^I and Pt^0–Pt^0 distances in molecules with d^{10} metals have been ascribed to such effects (Mehrohta & Hoffmann, 1978; Dedieu & Hoffmann, 1978).

The CaB_6 structure

This structure (15) was treated by Longuet-Higgins and Roberts in a pioneering paper twenty-five years ago (Longuet-Higgins & Roberts, 1954, 1955).

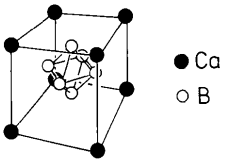

(15)

Our analysis of the parent system will then be rather cursory. Clearly the structure is built up from B_6 octahedra inserted into a primitive cube of metal atoms. One rather obvious difference to the cuprite structure is that the intraoctahedron B–B distances are similar to the interoctahedron distances between cells, the boron–metal distance is rather long and the metal is, in fact, twenty-four coordinate. The largest interactions are to be expected between octahedra, rather than as in the case of cuprite between the orbitals of the corner atoms and the inscribed polyhedron. For an n-vertex deltahedron there are $(n + 1)$ skeletal bonding orbitals (Stone, 1981) which, in the present case ($n = 6$), accommodate seven electron pairs. There are six electrons (three pairs) used in forming intercage B–B linkages. Of this total of twenty electrons, eighteen are formally contributed by the six boron atoms and two from the metal. The generation of the fragment-within-the-solid orbitals for the structure is shown in Fig. 12. Because the metal atom is located such a large distance from the boron atoms (3·054 Å in CaB_6) there is little direct covalent interaction between the two in our calculations. The small metal-level shifts, compared with those of B–B interactions, are not shown. A population analysis of the structure where metal and boron atoms have identical input atomic-orbital parameters is shown in (16) and clearly specifies the cage sites as those where the more electronegative atoms will lie. This arises simply because it is only the orbitals of the cage boron atoms which are significantly stabilized, and with a total of twenty electrons these deeper-lying orbitals are the ones which are occupied.

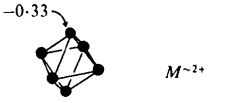

(16)

In molecular systems the structures of many polyhedral molecular species are governed by Wade's (1976) scheme, based on the $(n + 1)$ rule noted above. Thus $B_6H_6^{2-}$ contains an octahedron of boron atoms with a total of seven skeletal bonding pairs. Many molecular polyhedral systems are found which may be described as an octahedron of atoms with one (*nido*) or two (*arachno*) vertex atoms missing. Thus B_5H_9 has the structure (17) but still with a total of seven skeletal electron pairs. B_4H_{10} with the same number of skeletal pairs has the structure (18).

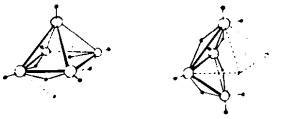

(17) (18)

In the language of the solid state this type of molecule could be regarded as a 'defect' octahedral molecule, just as $\square CdIn_2Se_4$ is a defect sphalerite superstructure. The theoretical reasoning behind the occurrence of these molecular and solid-state defect structures is similar (Burdett, 1979). We have performed a calculation on an MB_5 system to see if similar defect structures are possible in the solid state. The molecular-orbital analysis of the result is similar to that of the parent. The apical atom of the square-pyramidal B_5 unit now carries a lone pair of electrons and, as a population analysis indicates (19), the most electronegative cage atom should preferentially reside at this site (of lowest coordination number). The HOMO–

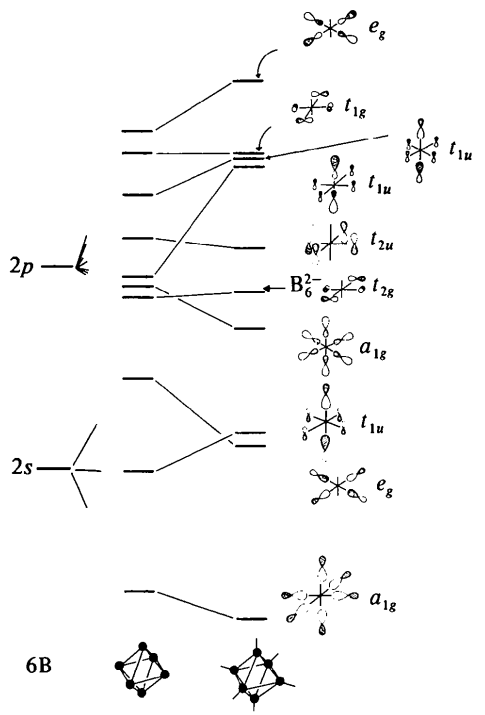

Fig. 12. The fragment-within-the-solid orbitals of CaB_6. The very small interaction with the orbitals located on the corner atom (Ca in CaB_6) is not shown. The dominant energetic effect is found between adjacent B_6 octahedra. Whether a particular orbital is stabilized or destabilized on including the cyclic boundary conditions to produce the fragment-within-the-solid orbitals is determined in every case (except the highest-lying e_g orbital) by the phases of the orbitals located *trans* to each other in the B_6 octahedron. Thus, a_{1g} orbitals are stabilized (bonding between adjacent B_6 units), t_{1u} orbitals are destabilized (dominated by σ contributions) *etc.* The largest energy changes are associated with the orbitals of σ type. The results are very similar to those derived from the band-structure calculations of Longuet-Higgins & Roberts (1954). They differ slightly in that these authors used identical Coulomb integrals for both boron 2*s* and 2*p* orbitals.

LUMO gap (calculated to be about 2 eV) is similar to that in CaB_6 itself and the structure is one that could exist for an $M^{IV}CB_4$ species containing an apical carbon atom.

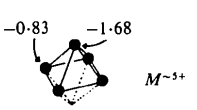

(19)

We thank the donors of the Petroleum Research Fund administered by the American Chemical Society for their partial support of this research.

APPENDIX

All our molecular-orbital calculations used the Extended Hückel method to derive both the level structures of the fragments and the band structure of the solid. The parameters are given in Table 1. The band-structure program was written by M.-H. Whangbo (and used in Whangbo, Hoffmann & Woodward, 1979), to whom we are grateful for permission to use it. The *s* orbital of the heavy central atom of the CsCl structure was contracted slightly so as to mimic the relativistic effects which are probably of importance at the bottom of the Periodic Table. The distortion (1 → 3) of the CsCl *AX* structure to that of red PbO used in the band-structure calculations was one which employed constant *AX* distances (of 1·8 Å).

One result which was parameter sensitive was the stability of the tetrahedral XA_4^{6+} fragments used to model the local *X* environment in alternatives to the red PbO structure. With the parameters of Table 1 the tetrahedral arrangement was found to be of lowest energy. With an uncontracted *s* orbital wavefunction the square-planar structure was more stable, a result not in accord with VSEPR theory. However, most systems for which the VSEPR approach is used do not usually consider as ligands electropositive atoms with a full complement of valence *s* orbitals. We do not know whether this is an artifact of our calculation method or a genuine manifestation of the contracted *s* orbital (inert-pair effect).

A word is in order concerning the population analyses presented in this paper. Invariably when the results of such an analysis are used in molecules, as in the SF_4 example, the ligand sites and *AX* linkages being compared are essentially similar, although symmetry inequivalent. Thus the axial and equatorial fluorine atoms in this molecular example are both one coordinate. In this paper we have extended the method to the solid state where we compare sites which may be rather different in nature. As a result, whereas the charges on the two types of fluorine atom in SF_4 are similar, we often find very different charges, in cuprite for example (13, 14), associated with the two different sites. There are also some other differences compared to the

Table 1. *Orbital parameters used in Extended Hückel calculations*

		H_{ii} (eV)	Exponent
$A^{(a)}$ (Pb)	3*s*	−15·0	1·783
A (Pb)	3*p*	−9·2	1·383
O	2*s*	−32·3	2·275
O	2*p*	−14·8	2·275
B	2*s*	−15·2	1·300
B	2*p*	−8·5	1·300
Cu	4*s*	−11·4	2·200
Cu	4*p*	−6·06	2·200
Cu	$3d^{(b)}$	−14·0	5·950 (0·5933), 2·300 (0·5744)

(*a*) A pseudo lead atom was used in the calculations on PbO with a contracted 3*s* function and increased H_{ii} to mimic the relativistic effect.
(*b*) This is in double ζ form with weighting coefficients in parentheses.

molecular case. Each fluorine atom in SF_4 contributes the same number of electrons to the molecular-orbital diagram. In Cu_2O each metal atom contributes one electron (from the s,p manifold) and each oxygen atom six electrons to give a total of eight electrons per formula unit. The charges depicted in (13) are therefore those of the atoms in the solid relative to neutral atoms with $\frac{8}{3}$ electrons, or in the sixteen-electron case of (14) with $\frac{16}{3}$ electrons per atom. A further consideration, also associated with the inequivalence of the atomic sites in the structures, is that the form of the molecular-orbital diagram for the case where all the atoms have the same atomic-orbital parameters should present the same molecular-orbital description as that for the real system where the parameters are different. This was found to be true for the CsCl → PbO transformation and also for the cuprite structure, but a problem arose with the CaB_6 structure. It should be recalled that the orbitals of the atoms of the primitive cube were virtually unchanged in energy on insertion of the B_6 octahedron. In the real structure of CaB_6 the calcium $3s$ orbital lies above the HOMO of the twenty-electron B_6^{2-} unit, but in the artificial structure where the atomic parameters of all the atoms are put equal then this nonbonding orbital lies just above the lowest-energy a_{1g} orbital of B_6 and of course will be filled in any *Aufbau* process. Not only is the resulting population analysis meaningless but with a total of twenty electrons the t_{2g} orbital contains only four electrons. The analyses presented in (16) and (19) are then somewhat artificial as far as the metal is concerned since in these cases we have adjusted its ionization potential so as to ensure that the t_{2g} orbitals are completely filled. The difference in site charges in (19), however, is a very real effect.

References

ANDERSSON, S. & ÅSTRÖM, A. (1972). *Natl Bur. Stand. US Spec. Publ.* No. 364, pp. 3–14.

BALDERESCHI, A. (1973). *Phys. Rev. B*, **7**, 5212–5215.

BARTELL, L. S. (1968). *J. Chem. Educ.* **45**, 754–767.

BURDETT, J. K. (1979). *Nature (London)*, **279**, 121–125.

BURDETT, J. K. (1980*a*). *Molecular Shapes*. New York: John Wiley.

BURDETT, J. K. (1980*b*). *J. Am. Chem. Soc.* **102**, 450–460.

BURDETT, J. K. (1980*c*). *J. Am. Chem. Soc.* **102**, 5458–5462.

BURDETT, J. K. (1981). *Structure and Bonding in Crystals*, edited by A. NAVROTSKY & M. O'KEEFFE. New York: Academic Press.

CHADI, D. J. & COHEN, M. L. (1973). *Phys. Rev. B*, **8**, 5747–5753.

COTTON, F. A. & WILKINSON, G. (1980). *Advanced Inorganic Chemistry*, 4th ed. New York: John Wiley.

DEDIEU, A. & HOFFMANN, R. (1978). *J. Am. Chem. Soc.* **100**, 2074–2079.

GIRICHEVA, N. I., ZASORIN, E. Z., GIRICHEV, G. V., KRASNOV, K. S. & SPIRIDONOVA, V. P. (1976). *Zh. Strukt. Khim.* **17**, 797–801.

HALPERN, J. (1968). *Adv. Chem. Ser.* No. 70, pp. 1–24.

HARRISON, W. (1980). *Electronic Structures of Solids*. San Francisco: Freeman.

HEINE, V. & WEAIRE, D. (1970). *Solid State Phys.* **24**, 249–463.

HOFFMANN, R. (1971). *Acc. Chem. Res.* **4**, 1–9.

HOFFMANN, R. (1981). *Science*, **211**, 995–999.

HOFFMANN, R., HOWELL, J. M. & ROSSI, A. R. (1976). *J. Am. Chem. Soc.* **98**, 2484–2492.

HOFFMANN, R. & LIPSCOMB, W. N. (1962). *J. Chem. Phys.* **36**, 2179–2189, 3489–3493; **37**, 2872–2883.

KETTLE, S. F. A. (1960). *Theor. Chim. Acta*, **4**, 150–154.

LONGUET-HIGGINS, H. C. & ROBERTS, M. DEV. (1954). *Proc. R. Soc. London*, **224**, 336–347.

LONGUET-HIGGINS, H. C. & ROBERTS, M. DEV. (1955). *Proc. R. Soc. London*, **230**, 110–119.

MEHROHTA, P. K. & HOFFMANN, R. (1978). *Inorg. Chem.* **17**, 2187–2189.

MESSMER, R. P., MCCARROLL, B. & SINGAL, C. M. (1972). *J. Vac. Sci. Technol.* **9**, 891–894.

MESSMER, R. P. & WATKINS, G. D. (1973). *Radiation Damage and Defects in Semiconductors*. Conf. Ser. No. 16, pp. 255–261. The Institute of Physics, London.

MINGOS, D. M. P. (1972). *Nature (London) Phys. Sci.* **236**, 99–102.

MINGOS, D. M. P. (1977). *Adv. Organomet. Chem.* **15**, 1–51.

PEARSON, R. G. (1969). *J. Am. Chem. Soc.* **91**, 1252–1254, 4947–4955.

PEARSON, R. G. (1970). *J. Chem. Phys.* **52**, 2167–2174; **53**, 2986–2987.

PEARSON, W. B. (1972). *The Crystal Chemistry and Physics of Metals and Alloys*. New York: John Wiley.

PITZER, K. S. (1979). *Acc. Chem. Res.* **12**, 271–276.

REITZ, J. R. (1955). *Solid State Phys.* **1**, 2–95.

ST JOHN, J. & BLOCH, A. (1974). *Phys. Rev. Lett.* **33**, 1095–1098.

STONE, A. J. (1981). *Inorg. Chem.* **20**, 563–571.

WADE, K. (1976). *Adv. Inorg. Chem. Radiochem.* **18**, 1–66.

WATKINS, G. D. & MESSMER, R. P. (1973). *Computational Methods for Large Molecules and Localized States in Solids*, pp. 133–147. New York: Plenum.

WELLS, A. F. (1975). *Structural Inorganic Chemistry*. Oxford Univ. Press.

WHANGBO, M.-H., HOFFMANN, R. & WOODWARD, R. B. (1979). *Proc. R. Soc. London Ser. A*, **366**, 23–46.

ZUNGER, A. (1974). *J. Phys. C*, **7**, 76–95, 96–106.

ZUNGER, A. (1975). *J. Chem. Phys.* **62**, 1861–1868; **63**, 1713–1731, 4854–4860.

ZUNGER, A. (1980*a*). *Phys. Rev. Lett.* **44**, 582–586.

ZUNGER, A. (1980*b*). *Phys. Rev. B*, **22**, 5839–5872.